JETIR.ORG ISSN: 2349-5162 | ESTD Year : 2014 | Monthly Issue
JOURNAL OF EMERGING TECHNOLOGIES AND INNOVATIVE RESEARCH (JETIR)
An International Scholarly Open Access, Peer-reviewed, Refereed Journal

DINUCLEAR COPPER(II) COMPLEXES WITH PENTADENTATE SCHIFF BASE LIGAND - SYNTHESIS, CHARACTERIZATION AND THEORETICAL EVALUATIONS.

S. PRAVEEN AND K. GEETHA*

PG & Research Department of Chemistry,
Muthurangam Government Arts College (Autonomous), Vellore, Tamilnadu, India.

Abstract

The growth of Schiff base-centered medicinal chemistry, together with the usage of less costly transition metals having strong pharmacological activity, has sparked a lot of interest in the creation of new Schiff base ligands. A new pentadentate Schiff base ligand 2,6-bis((E)-(2-amino-4-methylphenylimino)methyl)-4-methoxyphenol **(L1)** was synthesized from 4-methyl-orthophenlylenediamine and 2,6-diformyl-4-methoxyphenol. Two distinct Cu(II) Complexes (**C1 & C2**) were prepared using this ligand and various cu(II) precursor with different organic acids. The structure of the obtained Schiff base ligand **(L1)** and Copper(II) complexes **(C1 & C2)** is clarified using a variety of analytical techniques, including electronic spectroscopy, Fourier transform infrared spectroscopy, ^{1}H NMR, ^{13}C NMR spectroscopy, mass spectrometry, conductivity and magnetic susceptibility studies, which demonstrated the pentadentate chelation of the ligand. Extensive physical and theoretical investigations of the ligand (**L1**) were performed, and the results were compatible with the expected compositions. The electrostatic potential surface was mapped with different parameters, the HOMO-LUMO band gaps and Mulliken charges were determined. The results of the experiments and the theoretical DFT analysis coincide well. In addition, the binding interaction between the human estrogen receptor and the breast cancer-induced protein (PDB:3ERT) was examined in a molecular docking study of the Schiff base ligand **(L1)** and their Cu(II) complex **(C1)**.

Keywords: Schiff base ligand, DFT, HOMO – LUMO and Molecular Docking.

I.Introduction

By using heteroatom-containing organic ligands as coordination sites, coordination chemistry allows us to create a wide range of intriguing and practical complexes. Moreover, the ligands with multiple donor hetero atoms have drawn interest from all over the world in coordination chemistry due to their potent

chelating capacity to create mono, di, or multinuclear complexes (R. K. Mohapatra *et al.* 2014; 2011). Density functional theory (DFT)-based techniques have received a lot of interest especially in the area of quantum chemistry. DFT is able to provide data on the geometry, frontier molecular orbitals (FMO), electrical, and thermodynamic characteristics of the molecule in addition to its chemical behaviours. FMO analysis contributes significantly to quantum chemistry (Fleming 1976). It is significant for molecular interaction. Highest occupied molecular orbitals (HOMO) are the outermost orbitals that donate electrons, whereas the lowest vacant molecular orbital that accepts an electron is known as the lowest unoccupied molecular orbital (LUMO). Frontier Molecular Orbitals is another term for HOMO (FMO). The energy differential between the molecular orbitals has been found to have a major impact on molecules' optical, electrical, and chemical properties (Rajaei I *et al.* 2018). In the present, computer aided drug design (CADD) has become increasingly important in the creation of prospective medications to cure ailments. As comparison to traditional approaches, using CADD for drug development might result in lower costs and labour as well as a reduced development cycle (Y. Dahai *et al*. 2022). CADD encompasses a variety of techniques, including molecular docking, virtual screening, pharmacophore modelling, and dynamic simulation. These techniques are extensively used to invent, create, and evaluate pharmaceuticals and other physiologically active substances (Firoz A. Dain Md Opo *et al*. 2021). The most widely used method for creating biological and molecular processes to identify and simulate complex structures at the molecular or even atomic level is called molecular docking (L.L. Pares *et al.* 2022). This procedure starts with the aggregation of several ligand conformations at the receptor's active site, followed by a ranking of the ligands based on the energies of each specific binding conformation (Tiancheng Li *et al*. 2022).

II.Materials and Methods

2.1 Materials & Measurements

All of the chemicals used for synthesis of ligand and complexes were bought from Nice, TCL, SD Fine and Sigma Aldrich. They were analytical grade and were used as such. Using a Lambda-35 UV-Vis double beam spectrophotometer was used to record the UV – Visible spectrum of the ligand and complexes. Shimadzu's FT-IR spectrophotometer was employed to record FT-IR spectra in the 400 - 4000 cm^{-1} region using the KBr method. The conductance of the complexes was determined using an Equiptronics conductivity metre Model No. EQ-665 with a platinum electrode. Using DMSO-d6 as the solvent and TMS as the internal reference, the ligands' ^{1}H and ^{13}C-NMR spectra were obtained using a Bruker Advance II 400 MHz NMR instrument model. WATERS - XEVO G2-XS-QToF High-Resolution Mass Spectrometer was employed to record the molecular weight of the ligand and the complexes on LC-MS.

2.2 DFT Studies

The software programme Gaussian 09W was employed for all theoretical calculations. Using density functional theory (DFT) and the B3LYP (Becke's three parameter hybrid functional with Lee–Yang–Parr correlation functional, LYP) hybrid functional in conjunction with the 6-311++G(2d,P) basis set, molecular geometry optimisation of the compounds was carried out. The Gauss View 6.0.16 programme was accountable for creating the optimised molecular structures (R. Dennington *et al*. 2016).

2.3 Molecular docking

Molecular docking and visualisation analysis were carried out using the CDOCKER tool in Discovery Studio v3.5 (Accelrys, USA). The interaction energy, hydrogen bonds, binding energies, protein energy, and ligand-protein complex energy were used to calculate the ligand's binding affinity. The binding energy of CDOCKER is shown as negative score values. A higher (-) value energy signifies a higher required like-mindedness between the ligand and the receptor (A.Palaniammal *et al*. 2021).

2.4 Synthesis of Schiff base ligand (L1)

2,6-diformyl-4-methoxyphenol (10mmol; 1.8g) and 4-methyl-o-phenylenediamine (20mmol; 2.44g) were mixed in ethanol in a 1:2 ratio and thoroughly agitated in a magnetic stirrer for three hours. During the process, the solution's brown tint became golden yellow. TLC was used to monitor the reaction. After being repeatedly rinsed with ethanol, filtered, and dried, a solid that was golden yellow was developed.

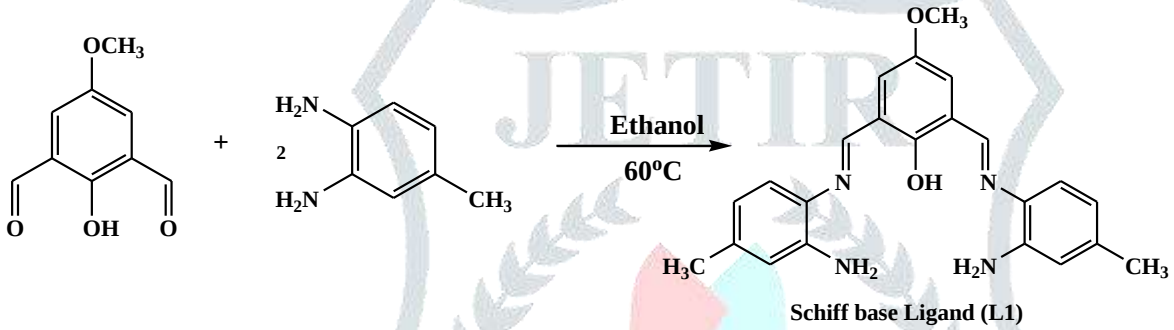

Scheme 1: Synthesis of Schiff base ligand (L1)

2.5 General method for preparation of copper(II) precursors

In order to synthesise the copper(II) precursors, benzoic acid and methyl benzoic acids were used. A solution of sodium hydroxide (50mmol; 2g) in water was gently added to benzoic acid (50mmol; 6.10g) had been dissolved in hot water. The aforesaid combination was added to copper(II) sulphate ($CuSO_4.5H_2O$) (25mmol; 6.24g). This mixture was then well stirred for an hour. The molar ratios of the organic acid, base, and copper(II) sulphate were 2:2:1 respectively. The obtained blue colour copper(II) precursors were carefully washed in water, then in ethanol, and finally dried.

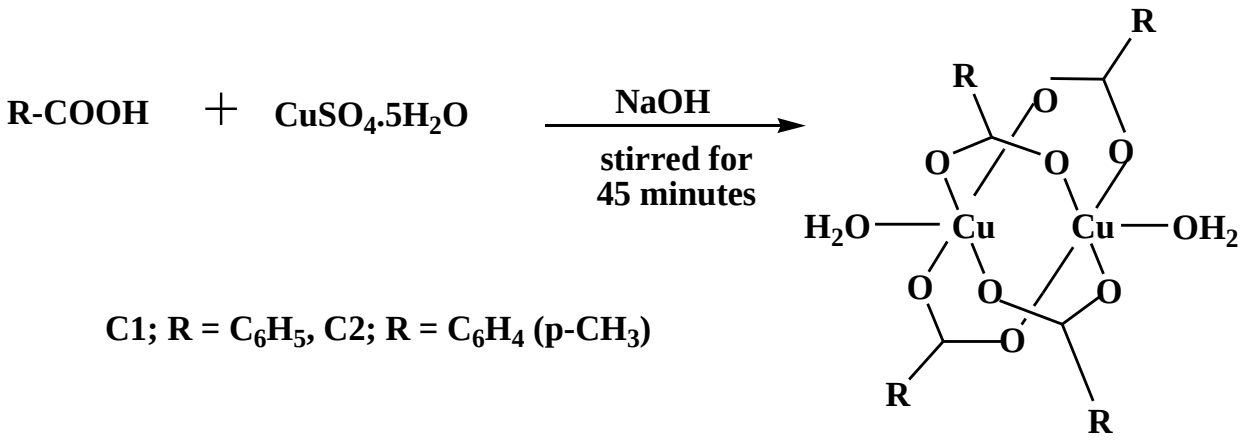

C1; R = C_6H_5, C2; R = C_6H_4 (p-CH_3)

Scheme 2: Preparation of copper(II) precursors.

2.6 General method for synthesis of copper(II) complexes

The Schiff base ligand (**L1**), NaOH, different copper(II) precursors, and $NaClO_4$ were used in the stoichiometric ratios of 1:1:1:2 to synthesise copper(II) complexes. A solution of sodium hydroxide (1mmol; 0.04g) was added to the dissolved Schiff base ligand (**L1**) (1mmol; 0.388g) and thoroughly swirled in a magnetic stirrer for 15 minutes to deprotonate it. Then slowly was added ethanol dissolved copper(II) precursor of benzoic acid (1mmol; 0.6475 g) to the aforementioned mixture. To this sodium perchlorate (2mmol; 0.28 g) was added and well agitated for five hours. The resultant crude product (**C1**) were subjected to several ethanol washes before being filtered and dried. Similar to this, the complex (**C2**) were synthesised using copper(II) precursors of methyl benzoic acid.

III.Results and Disscussion

3.1 Physico-Chemical properties

Table 1 lists the empirical formula, melting temperatures, yield and molar conductance values for Schiff base ligand (**L1**) and its associated copper(II) complexes. All of the complexes were revealed to exhibit molar conductivity values between 124 and 126 mho cm^2 mol^{-1}, and these results support the hypothesis that the novel complexes are 1:2 electrolytes (W. J. Geary 1971). The postulated stoichiometry of the novel compounds and the analytical findings are in good agreement.

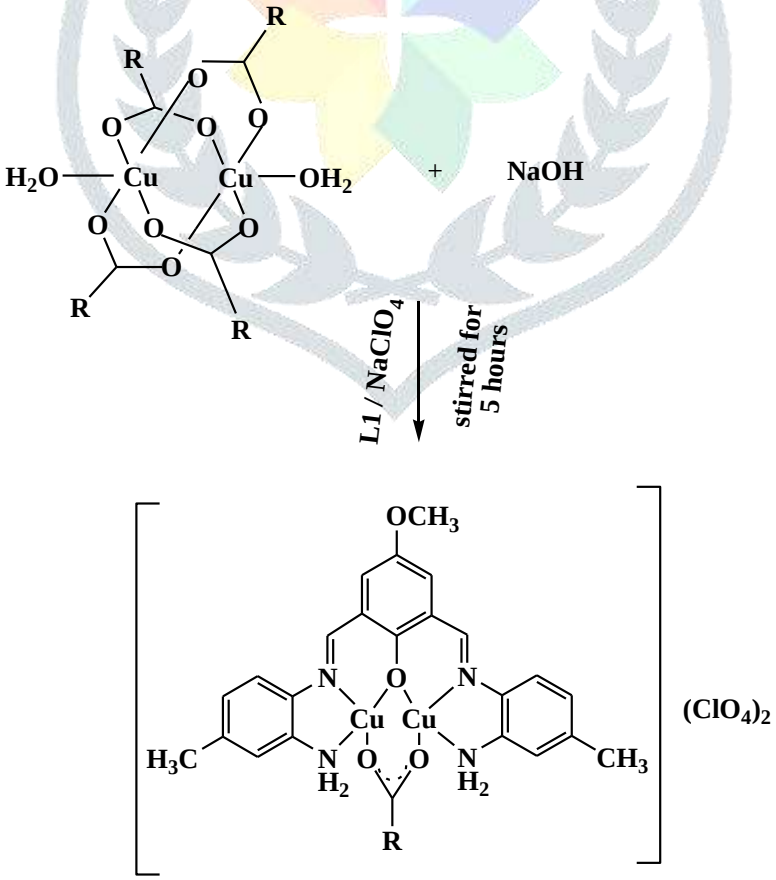

Copper(II) Complex

C1; R = C_6H_5,

C2; R = C_6H_4(p-CH_3)

Scheme 3: General scheme for synthesis of copper(II) complex.

Table 1: Physico-Chemical properties

Compound	Empirical Formula	melting point (°C)	Yield (%)	Molar Conductance (mho cm^2 mol^{-1})
L1	$C_{21}H_{20}N_4O_2$	248	80	-
C1	$C_{28}H_{24}Cl_2Cu_2N_4O_{12}$	>360	74	124
C2	$C_{29}H_{26}Cl_2Cu_2N_4O_{12}$	>360	76	126

3.2 Electronic spectra

The spectrum of the Schiff base ligand (**L1**) showed three absorption bands. The phenyl ring's absorption is attributed to the band at 294 nm whereas the second band at 365 nm corresponds to the azomethine group's π-π* transition. The third broad band at 423 nm was ascribed to n-π* transition of azomethine group. The electronic spectra of the complexes (**C1 & C2**) showed several absorption bands, including absorption bands of the ligands and d–d transitions of the metal ions. Spectrum of the complexes, which reveal maxima at the wavelength of the first band of the ligands at 298 – 299 nm are independent of complexation. The second bands for the complexes in the range 366 – 367 nm are evidently different for the second band of the free ligands, and there is an increase of absorption. The third band is endorsed to n-π* transitions involving the azomethine found at 432 – 434 nm (Manju et al. 2017). The band at 498 – 499 nm is assigned to ligand to metal charge transfer transition. Ligand to metal charge transfer are the outcome of an electronic transition from a filled orbital that is mostly based on a ligand to an empty orbital of the metal (Fabio Julia, 2022). Lower energy bands in the range 560 - 561 nm are assigned to d–d transitions of the copper ion.

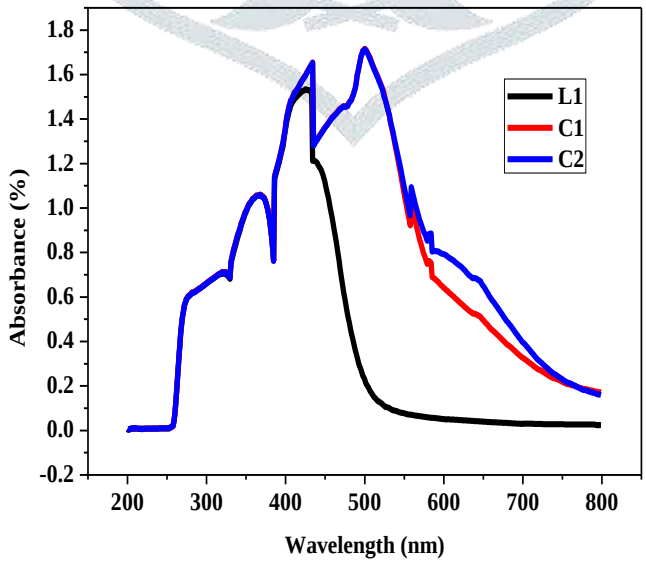

Figure 1: Electronic spectrum of L1, C1 & C2.

3.3 Vibrational Spectra

The peak in the 2950 cm^{-1} range is caused by the methyl group's aliphatic (C–H) stretching vibration in the benzene ring. This confirms a methyl group is present in the Schiff base Ligand (**L1**). As a result of the presence of hydroxyl groups in the Schiff base ligands, a distinctive wide band formed in the FT-IR spectra around 3100 cm^{-1}. This broad band disappears upon complexation, confirming the deprotonation of phenolic oxygen and its coordination with the central metal ions. The absorption band for the azomethine group (–HC=N–) was observed at 1622 cm^{-1}(L.J. Bellamy, 1969) and in metal complexes, this shifts to lower values by 10–20 cm^{-1}. At 1604–1616 cm^{-1} all complexes exhibit a peak for azomethine group. All the complexes had peaks in the 503 - 560 cm^{-1} and 426 - 465 cm^{-1} ranges, confirming the presence of (Cu-N)m(K. Nakamoto, 1978) and (Cu-O) (M. Shahid; 2017), respectively. In accordance with FT-IR measurements, the copper atoms in the complexes were coordinated via the oxygen atom of phenolic groups and the nitrogen atom of the azomethine group of Schiff base ligand.

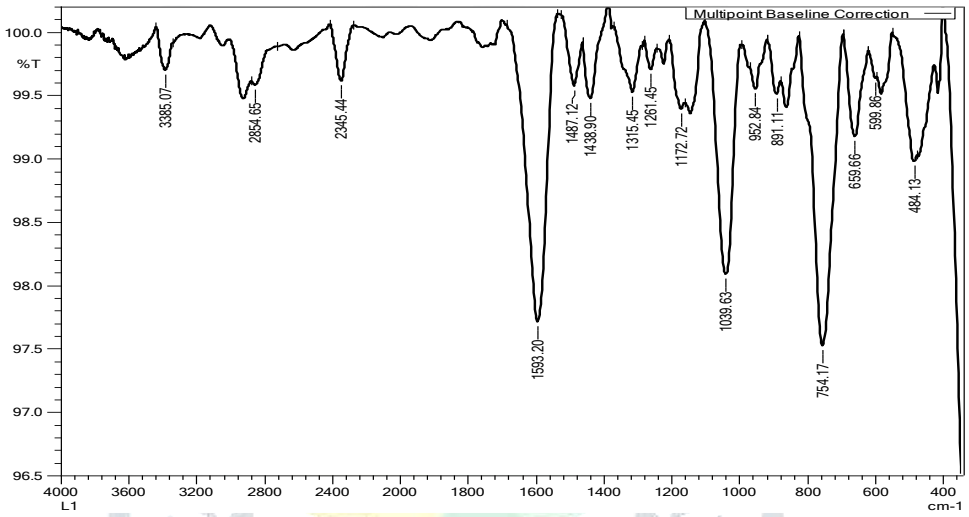

Figure 2: Vibrational spectrum of L1.

3.4 ^{1}H & ^{13}C NMR Spectra

In the ^{1}H NMR spectrum of Schiff base ligand (**L1**), a singlet signal appeared at 9.02 ppm is assigned to the azomethine group proton (M.S. Refat, et *al.* 2014). A multiplet appear in the region of 6.04 - 8.04 ppm is assigned for aromatic protons. The peak appeared at 13.58 ppm is evidence for the presence of phenolic OH proton. The signal appears at 4.3 ppm is assigned to the amino protons ($-NH_2$). The methyl protons appeared at 2.3 ppm (Ranjan K, et *al.* 2019) and the peak at 1.62 ppm are indexed to the methoxy ($-OCH_3$) proton respectively. ^{13}C NMR spectrum of synthesized Schiff base ligand (**L1**) showed a signal at 158 ppm due to azomethine group (Ashraf Sadat Ghasemi, et *al.* 2015). The chemical shift value of 155 ppm is due to hydroxyl group attached carbon atom. Aromatic carbon atoms in Schiff base ligand (**L1**) is attributed to the values in the range of 117-131ppm. The carbon atoms of the methoxy group ($-OCH_3$) is observed at 60 ppm. Methyl carbon atom in the Schiff base ligand (**L1**) is observed at 25.4 ppm.

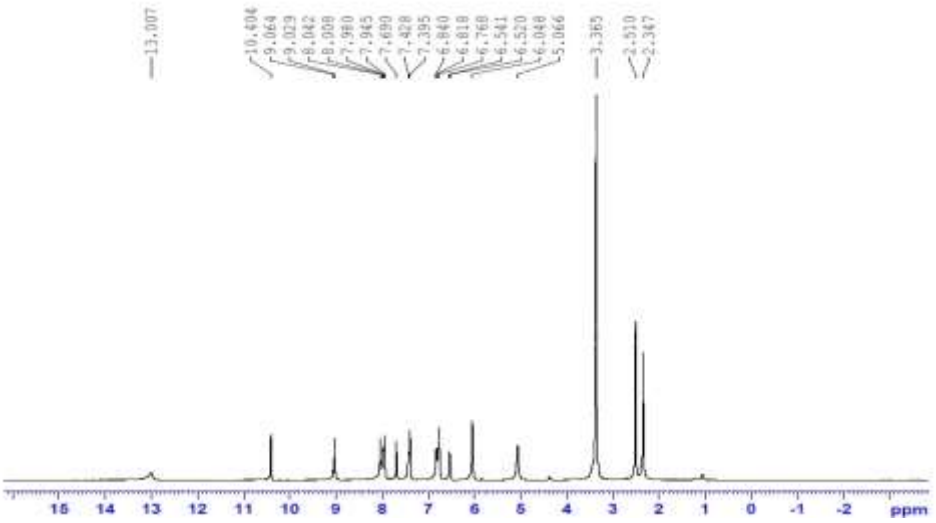

Figure 3: ^{1}H NMR Spectrum of L1.

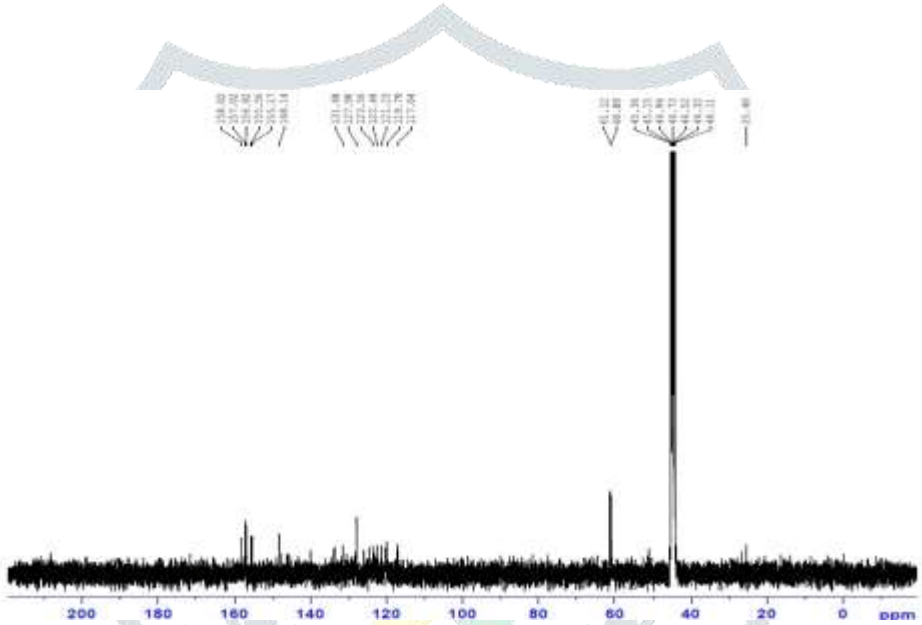

Figure 4: ^{13}C NMR Spectrum of L1.

3.5 Mass Spectra

The peak corresponds to (M+2) appear as molecular ion peak in the High Resolution Mass Spectra of the Schiff base ligand (**L1**) at m/z = 390.43 which exhibit the formation of Schiff base ligand with chemical formula $C_{23}H_{24}N_4O_2$. The molecular ion peak of synthesized copper(II) complex (**C1)** were observed at m/z 836.46 (M+2). Furthermore, the measured molecular mass of the synthesized complex **(C1)** spectra agrees with their proposed molecular structure with formula $C_{30}H_{28}Cl_2Cu_2N_4O_{12}$. The High Resolution Mass Spectra of the Schiff base ligand (**L1**) are given in Figure 5.

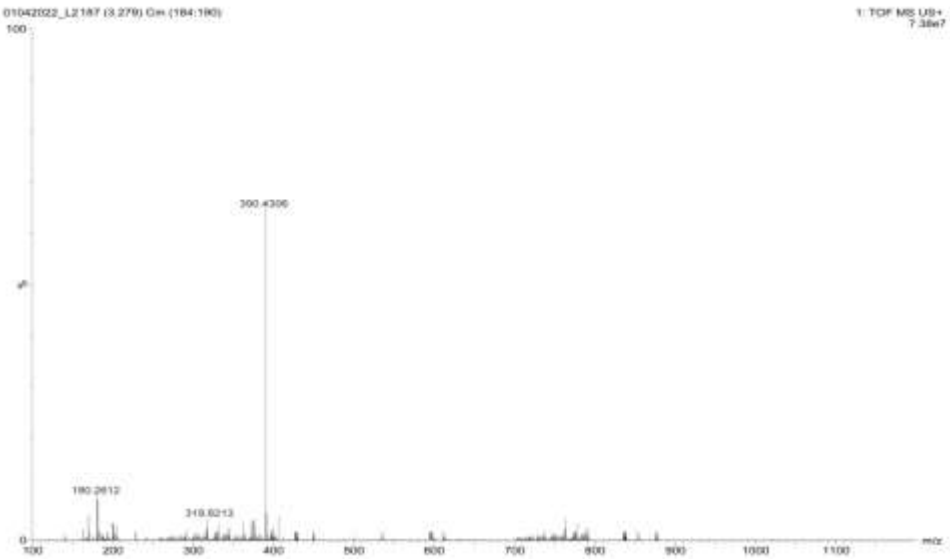

Figure 5: Mass spectrum of Schiff base ligand L1.

3.6 *In Silico* Studies

3.6.1 HOMO – LUMO

The molecule's electronic and reactivity properties are of great importance in various chemical interactions. The HOMO (Highest Occupied Molecular Orbital) and LUMO (Lowest Unoccupied Molecular Orbital) energy levels play a vital role in these interactions, with their values recorded at -5.0943 eV and -1.9375 eV, respectively for Schiff base ligand (**L1**). The energy gap between these levels, which measures 3.1568 eV, indicates the molecule's stability and reactivity, with a larger gap suggesting increased stability (Soltani A *et al.* 2015). The ionization potential, which equals the HOMO energy value, stands at 5.0943 eV, representing the energy needed to remove an electron from the molecule. The electron affinity, at 1.9375 eV (corresponding to the LUMO level), indicates the energy released when adding an electron. The molecule's electronegativity, calculated as 3.5159, showcases its ability to attract electrons during chemical bonding. The chemical potential, at -3.5159 eV, gives us an overall perspective of the electron potential energy. Additionally, the chemical hardness, measured at 1.5784 eV, and the chemical softness, at 0.3168 eV, offer information about the molecule's resistance to electron flow and its capability to either accept or donate electrons. As the predominant molecular orbital, the computed energy gap value indicates the ease of HOMO to LUMO electron excitation, which is consistent with the pentadentate ligand's overall nature as a strong electron donor with a high degree of nucleophilicity (Ismail Warad et *al.* 2020). In summary, this data provides a comprehensive understanding of the molecule's electronic structure and reactivity, which is vital for applications across the fields of chemistry, materials science, and beyond.

Table 2: Quantum molecular reactivity parameters of Schiff base ligand (L1).

Parameter	Values (B3LYP/6-311++G(d,p))
HOMO(eV)	-5.0943
LUMO(eV)	-1.9375
Ionization potential	5.0943
Electron affinity	1.9375
Energy gap(eV)	3.1568
Electronegativity	3.5159
Chemical potential	-3.5159
Chemical hardness	1.5784
Chemical softness	0.3168

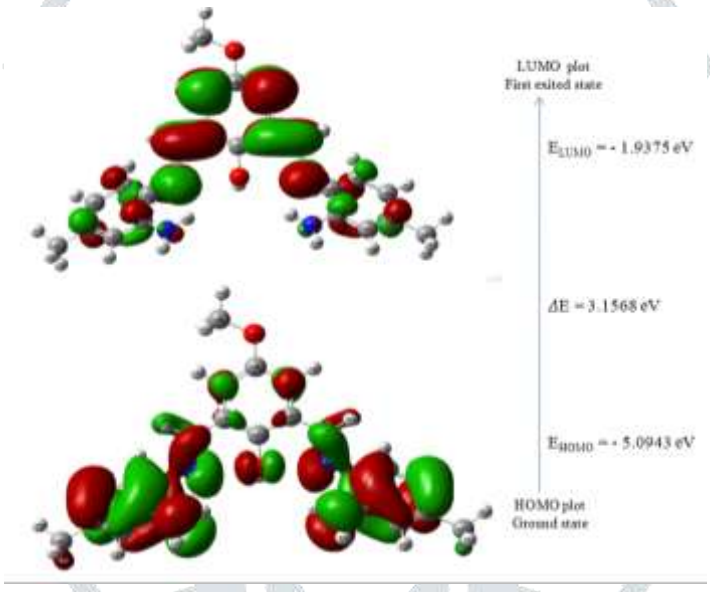

Figure 6: Plot of HOMO–LUMO and their energy gap for L1.

3.6.2 MEP (Molecular electrostatic potential)

For the molecule, 2,6-bis(E)-(2-amino-4-methylpenylimino)-4-methoxyphenol (**L1**). The molecular electrostatic potential (MEP) surface was determined by using the Gaussian 09W programme to optimise the checkpoint file at the B3LYP/6-311++(2d,p) level of DFT. The MEP maps are displayed in Figure 7. The majority of the positive and negative areas on the MEP surface are shown by the colours blue and red respectively, which represent for electron-rich and electron-deficient sites. The order in which the electrostatic potential increases is red < orange < yellow < green < blue (Aayisha, S et *al.* 2019).

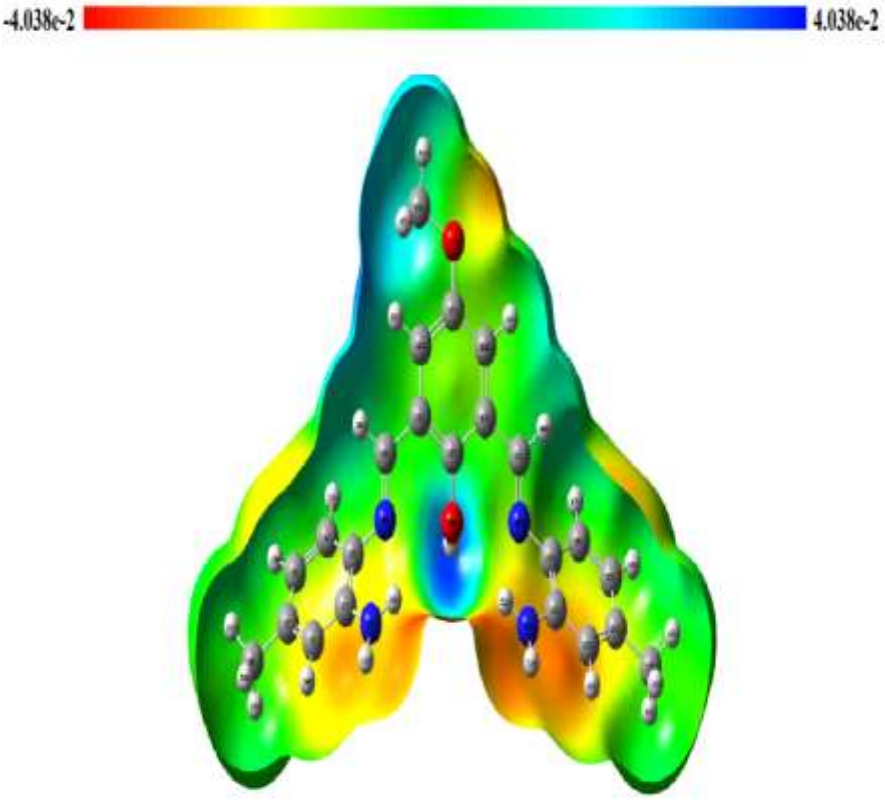

Figure 7: Molecular Electrostatic Potential mapping of L1.

3.6.3 Mulliken population analysis

The Mulliken atomic charges for2,6-bis(E)-(2-amino-4-methylpenylimino)-4-methoxyphenol (**L1**) are reported in Table 5. Where the atoms are numbered and the colour of the spheroids is shown in accordance with the partial atomic charge distributions shown in Figure 8. The higher basis set B3LYP/6-311++G(d,p) method is employed to produce a high degree of sensitivity. The charges of Hydrogen, Carbon, nitrogen and oxygen atoms are illustrated in the table 3.

Table 3: Atomic Charge of Schiff base ligand (L1).

Atoms	Charges	Atoms	Charges
1 N	-0.4044	**28 N**	-0.3974
2 C	0.0400	**29 O**	-0.0546
3 C	-0.1127	**30 H**	0.2912
4 C	-0.0240	**31 H**	0.2616
5 C	-0.6274	**32 H**	0.1408
6 C	0.4148	**33 H**	0.1485
7 C	-0.1426	**34 H**	0.1350
8 C	-0.4669	**35 H**	0.1682
9 N	0.1823	**36 H**	0.1320
10 C	-0.2190	**37 H**	0.1377
11 C	0.7711	**38 H**	0.1413
12 C	-0.5373	**39 H**	0.1854
13 C	0.8557	**40 H**	0.1313

14 C	-1.4014	**41 H**	0.1540
15 C	-0.9373	**42 H**	0.1560
16 C	0.0666	**43 H**	0.1918
17 O	-0.1538	**44 H**	0.1388
18 C	-0.3622	**45 H**	0.1337
19 C	0.1488	**46 H**	0.1472
20 N	0.1619	**47 H**	0.1423
21 C	-0.1951	**48 H**	0.1682
22 C	0.1459	**49 H**	0.1380
23 C	-0.2956	**50 H**	0.1322
24 C	0.4202	**51 H**	0.3096
25 C	-0.5371	**52 H**	0.2586
26 C	-0.1396	**53 H**	0.2956
27 C	-0.4378		

The maximum negative charge sharing was exhibited for nitrogen atom at different positions (1N, 28N) and the values obtained are -0.4044e, -0.3974e. The oxygen atoms obtained at (17O, 29O) -0.1538e, -0.0546e. The carbon atoms with positive charge were 2C (0.0400e), 11C (0.7711e), 16C (0.0666), 19C (0.1488e), 22C (0.1459e), 24C (0.4202e) Most of the hydrogen present in the 2,6-bis(E)-(2-amino-4-methylphenylimino)methyl-4-methoxyphenol (**L1**) exhibits high positive character especially hydrogen H30(0.2912e) attached with the oxygen atom exposed the most positive character, supporting the oxygen atom's electro negativity, and the result showed a strong association with MEP surfaces (Zhang S et *al.*; 2019).

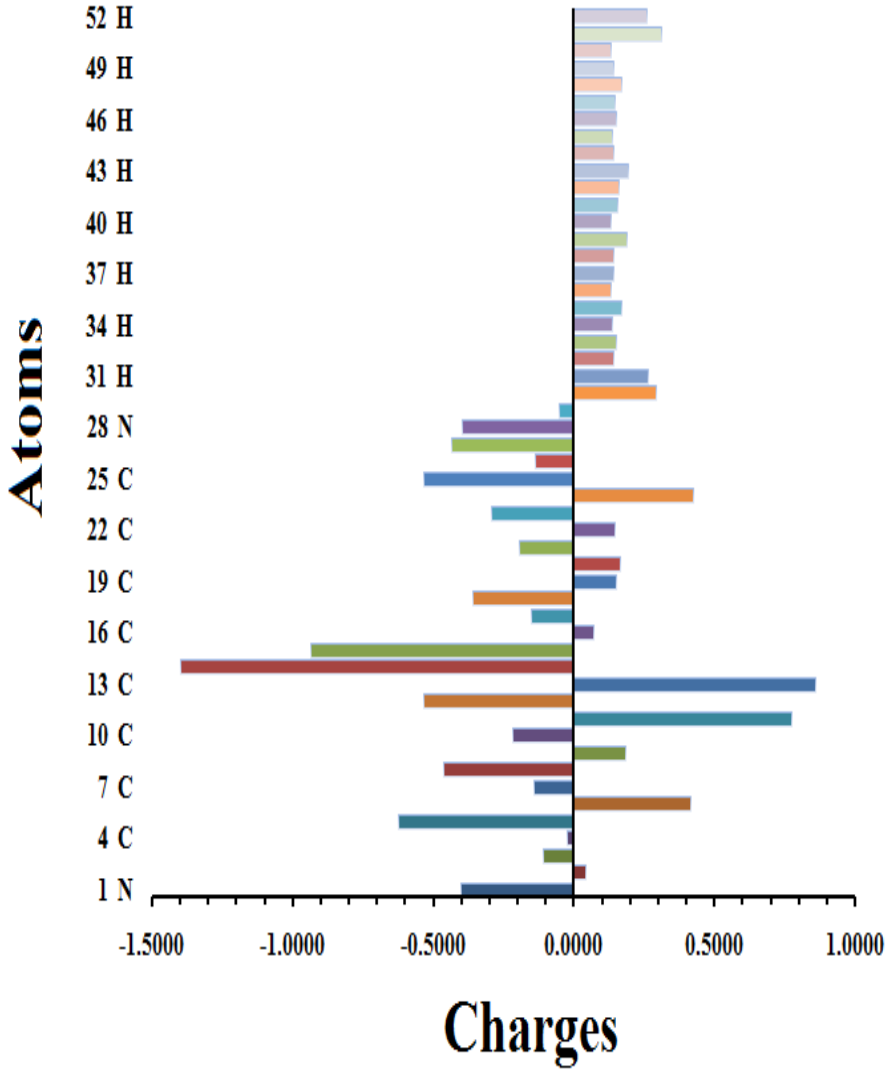

Figure 8: Mulliken Charge Plot of the Schiff base ligand L1.

3.6.4 Molecular docking

The Schiff base ligand (**L1**) shows the binding energy of -38.074 Kcal/mol. In this docking analysis, the primary amine group of the Schiff base ligand (**L1**) forms two strong H-bonding interactions with Asp 351 and Leu 346 amino acids respectively. The Trp 383 and Leu 536 amino acids show the π - π T-shaped and π - σ interactions respectively. Also other active site amino acids involved in the binding analysis by the alkyl, π - alkyl and Van der Waals interaction with the Schiff base ligand (**L1**) (Figure 9). Complex (**C1**) possesses a binding energy of - 48.4373 Kcal/mol. π - sulfur interactions linked the Cys530 residues to Complex **1**. The π - sulfur interaction with the Cu metal is observed in Asp 351 residues (Hwang et al., 2018). Complex 1's alkyl and aromatic group generate the non-bonded alkyl and π - alkyl interaction with the 3ERT receptor's active site amino acids (Figure 10).

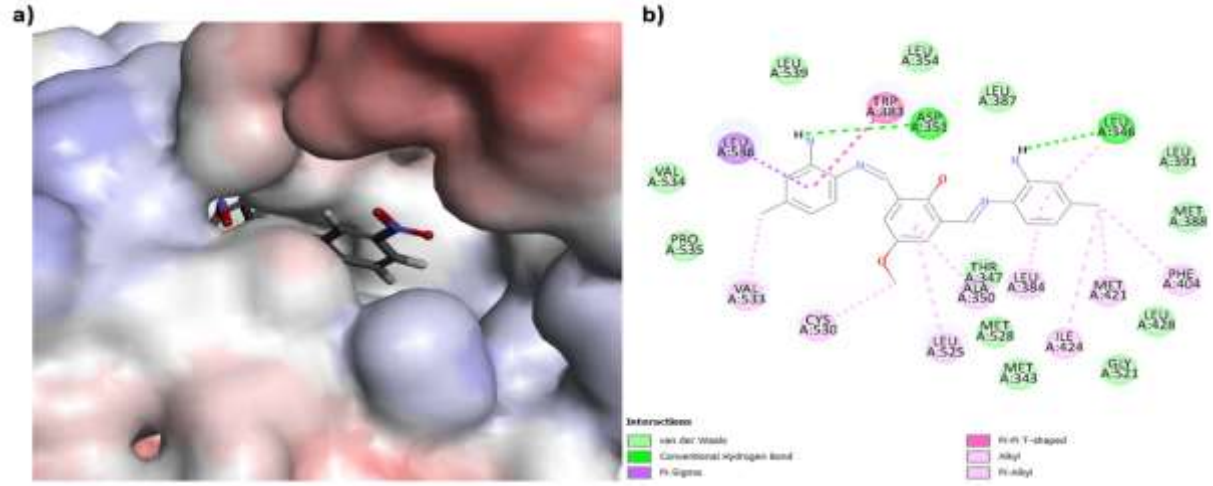

Figure 9: The a) 3D and b) 2D binding interactions of the L1 with 3ERT receptor.

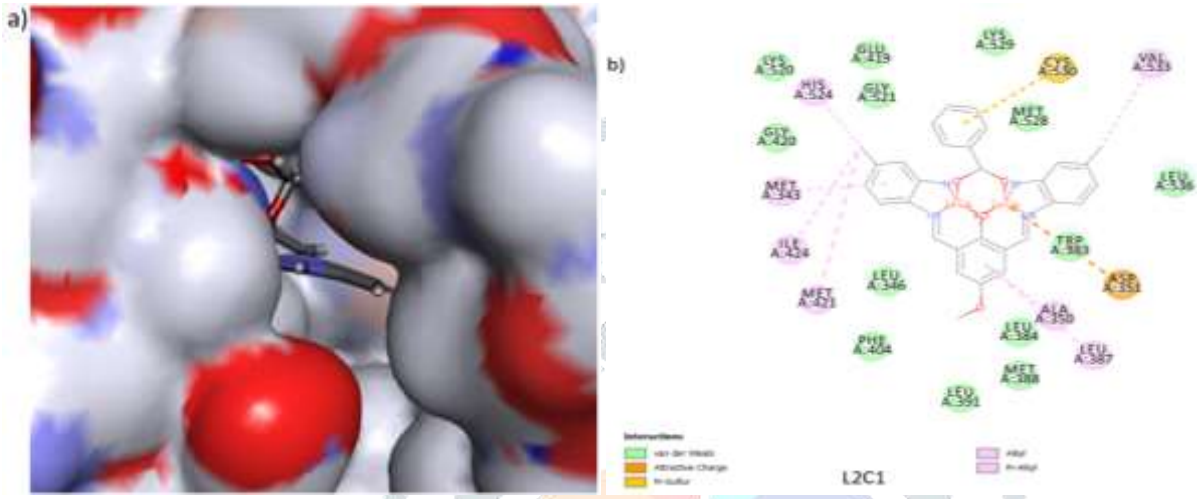

Figure 10: The a) 3D and b) 2D binding interactions of the C1 with 3ERT receptor.

IV. Conclusion

This present study involves a new pentadentate Schiff base ligand 2,6-bis((E)-(2-amino-4-methylphenylimino)methyl)-4-methoxyphenol synthesized from 4-methyl-orthophenlylenediamine and 2,6-diformyl-4-methoxyphenol. Two distinct Cu(II) Complexes were prepared using this ligand and various cu(II) precursor with different organic acids. The structure of the obtained Schiff base ligand and Copper(II) complexes was clarified using a variety of analytical techniques, including electronic spectroscopy, Fourier transform infrared spectroscopy, ^{1}H NMR, ^{13}C NMR spectroscopy, mass spectrometry, conductivity and magnetic susceptibility studies, which demonstrated the pentadentate chelation of the ligand. A prominent band in the FT-IR spectra at around 1600 cm^{-1} suggests a C=N bond. The mass spectrum showed the presence of a molecular ion at m/z=454.36 and m/z 835.67 which corresponds to the molecular weight of the synthesised Schiff base ligand and copper(II) complex, which has the chemical formula of $C_{23}H_{24}N_4O_2$, $C_{30}H_{28}Cl_2Cu_2N_4O_{12}$, respectively. The synthesis of the suggested compound was supported by ^{1}H and ^{13}C NMR. DFT analysis with B3LYP/6-31G(d, p) was performed, and the optimised geometry of the system was presented. The atomic charges of Mulliken and the HOMO-LUMO band gaps were also calculated. The molecular docking investigation of the Schiff base ligand and metal complexes for anticancer activity demonstrated that the synthesised compounds had an excellent binding relationship with anticancer receptors

when compared to the standard 5-fluorouracil. The study revealed that the active site of the residues created many bonded and non-bonded interactions between the metal complexes and the Schiff base ligand.

Reference

[1] A.M. Abu-Dief, I.M. Mohamed, Beni-Suef University Journal of Basic and Applied Sciences, 4, 133(2015) https:// 10.1016/j.bjbas.2015.05.004.

[2] A.Palaniammal and S. Vedanayaki, Rasayan J. Chem., 14 (5), 188-192, (2021) DOI: http://doi.org/10.31788/RJC.2021.1456733

[3] A.Soltani, R. Mashkoor, A. D. Khalaji, S. G. Raz, S. H. Ghoran, M. Dusek, K. Fejfarova & Y. Kanani Journal of Structural Chemistry, 60, 890–897 (2019) DOI: https://doi.org/10.1134/S0022476619060039

[4] Aayisha. S., Devi. T. R., Janani. S., Muthu. S., Raja. M., & Sevvanthi. S. Journal of Molecular Structure, 1186, 468–481, (2019) DOI: https://doi.org/10.1016/j.molstruc.2019.03.056

[5] Ashraf Sadat Ghasemi, Fereydoun Ashrafi, Javad Sharifi-Rad, Seyedeh Mahsan Hoseini Alfatemi, Cellular and molecular Biology, 61, 110-117, (2015) DOI: https://10.14715/cmb/2015.61.7.17

[6] C.A. Mebi, Journal of Chemical Sciences, 123, 731, (2011) DOI: https://10.1007/s12039-011-0131-2.

[7] D. Van Duin, D. Paterson, Infect Disease Clinics of North America 30, 390N, (2016) DOI:https://10.1016/j.idc.2016.02.004.

[8] Dr. Fabio Julia, The European society journal of catalysis, 14, Issue 19, (2022) DOI: https://doi.org/10.1002/cctc.202200916

[9] Firoz A. Dain Md Opo , M.M. Rahman, F. Ahammad, I. Ahmed, M.A. Bhuiyan and A.M. Asiri, Sci. Rep. 11, 4049 (2021). DOI: https://10.1038/s41598-021-83626-x.

[10] Fleming, Frontier Orbitals and Organic Chemical Reactions, Wiley, London (1976) DOI: https://doi.org/10.1002/prac.19783200525

[11] G. Wang, J.C. Chang, Synthesis and Reactivity in Inorganic and Metal-organic Chemistry, 24, 1097, (1994) DOI: 10.1080/00945719408001385.

[12] G.B. Deacon, R.J. Phillips, Coord. Chem. Rev. 33, 227–250, (1980) DOI: https://doi.org/10.1016/S0010-8545(00) 80455-5.

[13] H. Hrichi, N.A. Elkanzi, A.M. Ali and A. Abdou, Res. Chem. Intermed., 49, 2257 (2023) DOI: https://doi.org/10.1007/s11164-022-04905-4

[14] Ismail Warad, Hadeel Suboh, Nabil Al-Zaqri, Ali Alsalme, Fahad A. Alharthi, Meshari M. Aljohanie and Abdelkader Zarroukf, RSC Advances, RSC Adv., 10, 21806, (2020) DOI: https://10.1039/d0ra04323k

[15] K. Nakamoto, Infra-red and Raman Spectra of Inorganic and Coordination Compounds, third edition, John Wiley & Sons, New York, p. 112 (1978)

[16] L.J. Bellamy, Advances in Infrared Group Frequencies, Second ed., Mathuen, London, (1969)

[17] L.L. Pares, A.N. Canals, C. Avila and M.S.Martinez, Mar. Drugs. 20, 53 (2022) DOI: https://10.3390/md20010053.

[18] M. Shahid, A.S. Tasneem, M.N. Mantasha, F. Ahamad, K. Sama, Z.A.S. Fatma, Journal of Molecular Structure, 1146, 424–431, (2017) DOI: https:// dx.doi.org/10.1016/j.molstruc.2017.06.023

[19] M.S. Refat, M. Ali, Y. El-Sayed, A.M.A. Adam, J. Mol. Struct. 1038, 62–72, (2014) DOI: http://dx.doi.org/10.1016/j.molstruc.2013.01.059

[20] Manju, Neelima Mishra, and D. Kumar, Russian Journal of Coordination Chemistry, Vol. 40, No. 6, pp. 343–357, (2014) DOI: https://doi.org/10.1134/S1070328414050091

[21] N.A.A. Elkanzi, A.M. Ali, M. Albqmi and A. Abdou, Appl. Organomet. Chem., 36, e6868 (2022) DOI: https://doi.org/10.1002/aoc.6868

[22] R. Dennington, T.A. Keith and J.M. Millam, Gauss View,Version 6 (Semichem, Shawnee Mission, KS, (2016)

[23] R. Venkatesh, S. Renuka and I. Venda, Mater. Today Proc., 51, 1810,(2022)
DOI: https://doi.org/10.1016/j.matpr.2021.10.360

[24] Rajaei, I., Mirsattari, S.N., Journal of Molecular Structure 1163, 236–251 (2018)
DOI: https://doi.org/10.1016/j.molstruc.2018.02.010

[25] Ranjan K. Mohapatra, Ashish K. Sarangi, Mohammad Azam, Marei M. El-ajaily, Md Kudrat-E-Zahan, Suyanbhu B. Patjoshi, Dhruba C. Dash, Journal of Molecular Structure Journal, 1179, Pages 65-75, (2019)
DOI: https://doi.org/10.1016/j.molstruc.2018.10.070

[26] S.A. Matar, W.H. Talib, M.S. Mustafa, M.S. Mubarak, M.A. AlDamen, Arabian Journal of Chemistry,8, 857, (2015),
DOI: https:// 10.1016/j.arabjc.2012.12.039

[27] Tiancheng Li, R. Guo, Q. Zong and G. Ling, Carbohydrate Polymer, 276, 118644 (2022).
DOI: http://10.1016/j.carbpol.2021.118644

[28] V.S. Mironov, T.A. Bazhenova, Yu.V. Manakin, K.A. Lyssenko, A.D. Talantsev and E.B. Yagubskii, Dalton Trans., 46, 14083 (2017)
DOI: https://doi.org/10.1039/C7DT02912H33.

[29] W. J. Geary, Coord. Chem. Rev., 7, 1971, 81-122
DOI: https://doi.org/10.1016/S0010-8545(00)80009-0

[30] W. Wang, F.-L. Zeng, X. Wang and M. Tan, Polyhedron, 15, 1699, (1996)
DOI: https://doi.org/10.1016/0277-5387(95)00403-3

[31] Y. Dahai, L. Wang and Y. Wang, Int. J. Mol. Sci. 23, 4738, (2022)
DOI: https://10.3390/ijms23094738.

[32] Y.A. Alghuwainem, H.M. Abd El-Lateef, M.M. Khalaf, A.A. Abdelhamid, A. Alfarsi, M. Gouda, M. Abdelbaset and A. Abdou, J. Mol. Liq., 369, 120936 (2023)
DOI: https://doi.org/10.1016/j.molliq.2022.120936

[33] Z.H. Chohan, M. Arif, M. Sarfraz. M. Applied Organometallic Chemistry, 21, 302(2007), DOI:http://10.1002/aoc.1200.